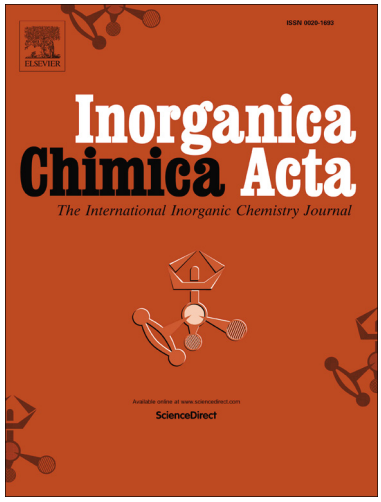

Research paper

Synthesis, structural and magnetic characterizations of a dinuclear copper(II) complex with an (N,S,O) donor ligand: catecholase and phenoxazinone synthase activities

Ayon Kanti Ghosh, Anzar Ali, Yogesh Singh, Chandra Shekhar Purohit, Rajarshi Ghosh

PII: S0020-1693(17)31838-8
DOI: https://doi.org/10.1016/j.ica.2018.02.004
Reference: ICA 18113

To appear in: *Inorganica Chimica Acta*

Received Date: 2 December 2017
Revised Date: 31 January 2018
Accepted Date: 1 February 2018

Please cite this article as: A.K. Ghosh, A. Ali, Y. Singh, C.S. Purohit, R. Ghosh, Synthesis, structural and magnetic characterizations of a dinuclear copper(II) complex with an (N,S,O) donor ligand: catecholase and phenoxazinone synthase activities, *Inorganica Chimica Acta* (2018), doi: https://doi.org/10.1016/j.ica.2018.02.004

Synthesis, structural and magnetic characterizations of a dinuclear copper(II) complex with an (N,S,O) donor ligand: catecholase and phenoxazinone synthase activities

Ayon Kanti Ghosh[a], Anzar Ali[b], Yogesh Singh[b], Chandra Shekhar Purohit[c], Rajarshi Ghosh[a,*]

[a]Department of Chemistry, The University of Burdwan, Burdwan 713 104, India

[b]Department of Physical Sciences, Indian Institute of Science Education & Research, Mohali, Sector 81, S. A. S. Nagar, Knowledge City, Manauli PO, Mohali, 140 306, India

[c]School of Chemical Sciences, National Institute of Science Education & Research, Bhubaneswar, Orissa, 751 005,India

Abstract

A new dinuclear Cu(II) complex (**1**) was synthesized and crystallographically characterized. Each of the Cu(II) centres has penta coordination and been found to adopt square pyramidal geometry. Variable temperature magnetic measurements showed that there is weak ferromagnetic interaction between the Cu(II) centres in **1**. **1** shows catecholase as well as phenoxazinone synthase activities in different solvents. The turn over numbers for the catecholase activity were 4.02×10^3 h^{-1} (MeOH) and 9.57×10^3 h^{-1} (MeCN), and that of phenoxazinone synthase activity were 1.065×10^3 h^{-1} (MeOH), 2.13×10^2 h^{-1} (MeCN) and 2.844×10^3 h^{-1} (DCM).

Keyword: Copper, Schiff base, catecholase activity, phenoxazinone synthase activity

*Corresponding author, E. mail: rghosh@chem.buruniv.ac.in

1. Introduction

Copper containing proteins are well known redox catalysts in different biological processes. These copper proteins are classified as type-1, type-2 and type-3 based on their spectroscopic features [1a]. Catechol oxidase is a type 3 copper protein and is found in plants. Catalysis of catechol-quinone oxidation reactions by catechol oxidase in presence of aerial oxygen is known as catecholase activity [1]. The resulting quinones auto-polymerize to give brown pigments which are responsible to defend the damages caused by pathogens and insects to plants. As soon as the active site structure of catechol oxidase appeared in literature [3] as an antiferromagnetically coupled dinuclearcopper(II), a number of groups around the world started to report [4-6] different Cu(II) and other transition metal complexes as structural and/or functional model for catecholase activity (Scheme 1). Phenoxazinone synthase [1b, 2], which is an another multicopper enzyme, is naturally produced by *Streptomyces antibioticus*. The active site structure of phenoxazinone synthase as hexameric copper complex appeared in literature in 2006 [8]. This is responsible for six electron oxidative coupling of two molecules of an *o*-aminophenol (OAPH) to form the phenoxazinone chromophore (Scheme 2) [2, 9, 10]. Metal complexes of different (N,N), (N,O) and (N,S) donor ligands, which exhibit catecholase and phenoxazinone synthase activities, are there in literature [4-7, 9, 10]. Use of different donor groups in the ligand backbone, which ligates to the metal with different strengths, helps to attack substrates by opening their donor site(s) with different extents leading to increased or decreased catalytic rates. In this endevour, we have synthesized a new (N,S,O) donor organic ligand having mixed soft-hard donor sites and its ferromagnetically coupled dichloro bridged dinuclear Cu(II) complex. The metal complex $[Cu_2^{II}L_2Cl_2]$ (**1**) [HL = 2-((*E*)-(2-

(benzylthio)ethylimino)methyl)phenol] is X-ray crystallographically and magnetically characterized. It mimics the activities of catechol oxidase as well as phenoxazinone synthase in different solvents. The mechanistic pathway for these activities are tried to be enumerated. Here to note, in spite of our best effort, we have not found any metal system complexed with (N,S,O) donor ligand.

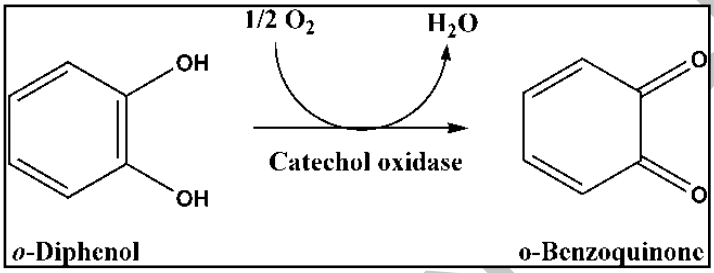

Scheme 1. Catecholase activity

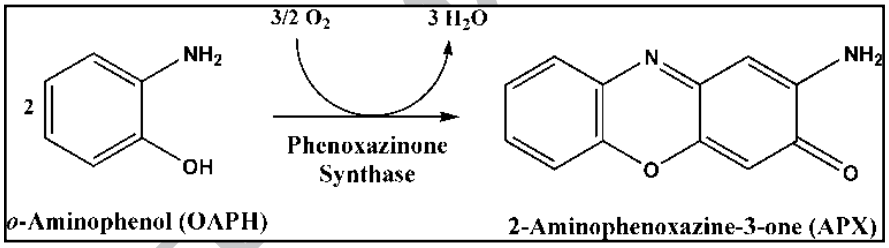

Scheme 2. Phenoxazinone synthase activity

2. Experimental

2.1.Materials

High purity benzylmercaptan, 2-chloroethylamine, salicylaldehyde and Copper(II) chloride dehydrate were purchased from Sigma Adrich, India. Ethanol and methanol were used as reagent grade solvents. 3,5-di-tert-butylcatechol was purchased from Sigma Aldrich, India and 2-aminophenol was purchased from Loba Chemie.

2.2. Physical measurement

Elemental analyses (carbon, hydrogen and nitrogen) were performed on Perkin-Elmer 2400 CHNS/O elemental analyzer. UV-VIS and IR spectra (KBr discs, 4000-300 cm^{-1}) were recorded using a Shimadzu UV-VIS 1800 spectrophotometer and Perkin-Elmer FT-IR model RX1 spectrometer, respectively.

2.3. Synthesis of HL

The synthesis of ligand HL is depicted in Scheme 3. Sodium ethoxide was prepared *in situ* by addition of pinch of metallic sodium in dry ethanol. Benzyl mercaptan (8 mmol, 0.99 g) was added to sodium ethoxide solution by stirring. Then 2-chloroethylamine (8 mmol, 0.63 g) was added slowly to the reaction mixture and stirred for about 1 hour. The precipitation of sodium chloride confirms the formation of the 2-(benzylthio)ethanamine (Scheme 3). This product was characterized by ^{1}H NMR (δ (ppm): 1.75 (t, J = 7.6 Hz, 2H), 2.81 (t, J = 6.8 Hz, 2H), 3.14 (t, J = 6.8 Hz, 2H), 3.60 (s, 2H), 7.25-7.33 (m, 5H)). (Fig. S1; Supporting information) and high resolution mass spectrometry (m/z= 168.0927) (Fig. S2; Supporting information). Sodium chloride was separated by filtration. Addition of salicylaldehyde (8 mmol, 0.97 g) to this solution of 2-(benzylthio)ethanamine with six hour reflux gives the ligand HL. Yield: (based on salicylaldehyde) 1.56 g (72%). Anal. calc. for $C_{16}H_{17}NOS$ (**HL**): C, 70.81; H, 6.31; N, 5.16; Found: C, 70.79; H, 6.33; N, 5.18 and high resolution mass spectrometry (m/z = 296.0271) Selected IR bands (cm^{-1}): 698, 756, 1028, 1278, 1452, 1492, 1629. UV-Vis (λ, nm): 254 (ε = 2863 $M^{-1}cm^{-1}$), 313 (ε = 945 $M^{-1}cm^{-1}$), 389 (ε = 300 $M^{-1}cm^{-1}$).

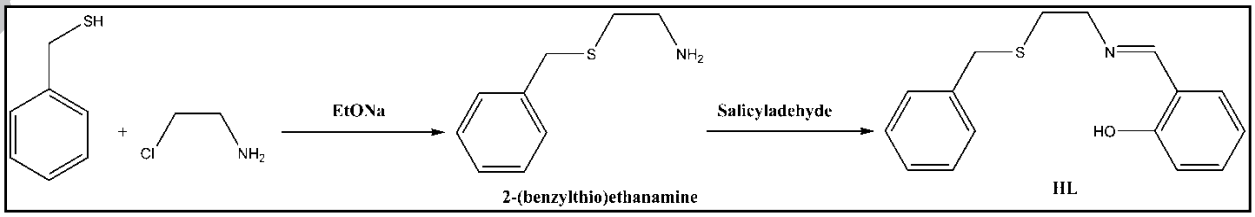

Scheme 3

*2.4. Synthesis of compound **1***

Compound **1** was prepared by drop-wise addition of copper(II) chloride dihydrate (0.370 g, 1 mmol) solution in ethanol (15ml) into a stirring ethanolic solution of HL(0.271g, 1 mmol). The yellowish ligand solution was turned green after addition of copper(II) salt. Then the reaction mixture was filtered and kept in air for slow evaporation. After about 60 days, the greenish coloured shiny square shaped crystals of X-ray quality of **1** was collected, washed with hexane and dried *in vacuo* over silica gel indicator.

Yield: (based on metal salt) 0.554 g (75%). Anal. calc. for $C_{32}H_{32}N_2O_2S_2Cl_2Cu_2$ (**1**): C, 52.03; H, 4.34; N, 3.79; Found: C, 52.01; H, 4.29; N, 3.82. Selected IR bands (cm^{-1}): 1620, 1028. UV-Vis (λ, nm): 238(ε = 34180 $M^{-1}cm^{-1}$), 271 (ε = 21900 $M^{-1}cm^{-1}$), 323 (ε = 9020 $M^{-1}cm^{-1}$), 371 (ε = 6140 $M^{-1}cm^{-1}$), 644 (ε = 360 $M^{-1}cm^{-1}$).

2.5. X-ray diffraction study

Single crystals of **1** were collected and selected for single crystal X-ray diffraction. Single crystal X-ray diffraction data were collected on collected on a Bruker AXS KAPPA APEX II diffractometer using Mo-K_α radiation (λ = 0.71073 Å) at 293(2) K. Systematically absent reflections led to the identification of space groups *P121/n1* for **1**. Of the 16850 total reflections for the complex, 4882 with [I >2r(I)] were used for structure solutions. The structures were solved by direct methods, and the structure solution and refinement were based on $|F^2|$. All non-hydrogen atoms were refined with anisotropic displacement parameters whereas hydrogen atoms were placed in calculated positions when possible and given isotropic U values 1.2 times that of the atom to which they are bonded. The final differences Fourier map showed the maximum and minimum peak heights at 0.463 and -0.6590 $eÅ^{-3}$ for **1** with no chemical significance. All

calculations were carried out using SHELXL-97 [11] and ORTEP-32 [12]. The crystal data and data collection parameters are listed in Table 1.

3. Results and discussion

3.1. Synthesis and formulation

The ligand was synthesized in two steps. In the first step, the thiol group of benzylmercaptan was deprotonated using sodium ethoxide which was generated *in situ*. Nucleophilic attack at 2-chloro carbon in 2-chloroethylamine was done by that deprotonated benzyl mercaptan (Scheme 3). The resulting 2-(benzylthio)ethanamine was characterized by proton NMR spectroscopy and mass spectrometry. The signals for the amine protons of 2-(benzylthio)ethanamine appeared at δ 1.75 (t, J = 7.6 Hz, 2H). The two triplet signals for four protons of the two methyl groups were found at δ 2.81 (t, J = 6.8 Hz, 2H) for one methylene group β to amine group and δ 3.14 (t, J = 6.8 Hz, 2H) for another methylene group α to the NH_2 group. The signal appeared at δ 3.60 (s, 2H) due to the methylene group which is α to the C-S bond. The signals of the five aromatic protons were appeared at the range between δ 7.25 ppm to δ 7.33 ppm (m, 5H). The molecular ion peak of 2-(benzylthio)ethanamine in HRMS appeared at m/z = 168.09 which is the molecular weight of the compound. This 2-(benzylthio)ethanamine was condensed with salicyaldehyde to get the ligand HL. The HRMS of sodium aggregate of HL appears at m/z = 296.02 (Fig. S3; Supporting information), and IR and UV-Vis spectroscopic data were collected to characterize this. Ethanolic mixture of copper(II) chloride dihydrate and HL resulted the dinuclear complex **1**. X-ray crystallographic characterization of **1** was done to know exact coordination sphere. IR spectrum of **1** shows sharp peaks among which peaks at 1028 and 1620 cm^{-1} were identified as Cu-O stretch in the complex and imine stretch of the

corresponding ligand [13]. Electronic spectrum of **1** was measured in methanol. It displays a d-d transition band at 644 nm and a $OH^- \rightarrow$ Cu(II) charge transfer band at 323 nm and 371 nm [14].

3.2. X-ray structure

The ORTEP of the complex is given in Fig. 1. The Molecular unit contains dichloro bridged dinuclearcopper(II) centres. Each of the copper(II) centres is five coordinated. Calculation of $\tau = 0.24$ [15] suggests that the metal centre is in square pyramidal geometry. From consideration of bond angle and bond distance data O(1) (phenolic oxygen), N(1) (imine nitrogen) and S(1) (thio ether sulfur) from the ligand network and Cl(1) (one of the bridging chlorides) are in the square plane. The bond distance range in the basal plane is 1.8920(18) to 2.815 Å. The another chloro bridge Cl(1') having larger bond distance than the other four are in the axial position.

3.3. Magnetism

Magnetic susceptibility χ versus temperature T measurements were performed on powder samples in an applied magnetic field of H = 1 T, using the VSM option of a Quantum Design PPMS.

The χ(T) vs T data are shown in Fig. 2. To extract the nature and magnitude of magnetic interactions in the system we have first analyzed the χ(T) data using the Curie-Weiss model for which the susceptibility in the paramagnetic state is given by the expression $\chi = \chi_0 + C/(T - \theta)$, where χ_0 is the temperature independent contribution, C is the Curie constant which depends on the effective magnetic moment, and θ is the Weiss temperature, the sign and magnitude of which will give the nature of the magnetic exchange interactions. For small χ_0, this will lead to $1/\chi$(T) being linear. The $1/\chi$(T) vs T data above T = 150 K are shown in the inset (I) of the figure. It can

be seen that at high temperatures, the behavior is linear as expected. These data were fit to the above Curie-Weiss expression. The parameters obtained from the fit are χ_0 = -9.17(3) × 10^{-5} cm^3/Cu mol, C = 0.382(3) cm^3/Cu mol K, and θ = 17.1(9) K. From C, the effective moment μ_{eff} can be estimated using the expression $C = N_A\mu^2_{eff}/3k_BT$, where N_A is the Avogadro's number and k_B is the Boltzmann constant. This gives μ_{eff} = 1.75(2) μ_B which is close to the value expected for S = ½ magnetic moments is μ_{eff} = 1.73 μ_B assuming a *g*-factor of g = 2. This fit is shown as the red curve through the data in inset **I** of Fig. 2.

Let us now turn to the nature of the magnetic exchange interactions between these S = ½ Cu(II) moments. The value θ = 17.1 K indicate moderate ferromagnetic coupling between the Cu(II) ions. Evidence for this can also be seen in the χT data which is shown in inset **II** of the Fig. 2. χT, which is roughly the effective moment, is weakly T-dependent for higher temperatures but increases dramatically as the temperature is lowered towards T = θ. Normally, the system would undergo long-ranged ferromagnetic transition at this temperature. However, our system is built up of Cu-Cu dimers which are isolated from each other and are expected to be interacting very weakly with each other.

We have thus tried fitting our χT data using a model of non-interacting S = ½ dimers. The magnetic susceptibility χ(T) for a collection of non-interacting S = ½ dimers with intra-dimer coupling J_1 can be written as

$$\chi_D(T) = \left(\frac{2N_A\mu_B^2 g^2}{k_B T}\right)\left[\frac{3}{3+3e^{\frac{J_1}{2T}}}\right].$$

Assuming that the interactions between dimers acts as a mean-field, the susceptibility of interacting dimers can then be written as

$$\chi_{in}(T) = \left(\frac{\chi_0}{1+\lambda\chi_0}\right)$$

Where λ is the exchange coupling which can be given in terms of the inter-dimer exchange J_2 as $\lambda = J_2/3C$, where C is the Curie constant for a S = ½. In addition to the contribution from dimers, there could be other core and paramagnetic impurity contributions. The experimental χ(T) data were therefore fit by the expression

$$\chi(T) = \chi_0 + \frac{C_{imp}}{T-\theta_{imp}} + \chi_{int},$$

Where, χ_0 is a T independent of temperature C_{imp} is the Curie constant of impurity spins, and θ_{imp} is the Weiss temperature giving interactions between these impurity spins. The fit, shown in Fig.1 as the red curve through the data in the main panel and in inset (II) gave the values χ_0 = -6.4(7) × 10^{-5} cm^3/Cu mol, C_{imp} = 0.0013(3) cm^3/Cu mol K, θ_{imp} = -0.24(1) K, J_1 = 16.8 (1) K and J_2 = -0.50(5) K. The error factor came out to be R = 2.07 × 10^{-5}. The small values of C_{imp} and θ_{imp} indicate that paramagnetic impurities, if present, are in small numbers and are almost non-interacting. The value J_1 = 16.8 K shows the presence of ferromagnetic interactions within Cu-Cu dimers and the small value of J_2 = -0.5 K suggests very weak antiferromagnetic interactions between dimers.

*3.4. Catecholase activity of **1**:spectrophotometric study*

In order to study the catecholase activity, 3,5-ditertiarybutylcatechol (3,5-DTBC) was chosen as a substrate. It can easily be oxidized to the corresponding quinone 3,5-ditertiarybutylquinone (3,5-DTBQ) which is very stable because the low quinine catechole reduction potential. Before proceeding the detail kinetic experiment we have done simple repetitive UV-VIS scan for 6 hours by adding the mixture of the catalyst (1 × 10^{-4} M concentration) and 100 equivalent amount of the substrate 3,5-DTBC in methanol and acetonitrile solvents (Figs. 3 and 4). 3,5-DTBC shows a single band at 282 nm (inset to Fig. 3). Characteristic peaks of 3,5-DTBQ, which is an oxidation product of 3,5-DTBC by aerial oxygen

in presence of **1**, appears at 398 nm in methanol and 401 nm in acetonitrile are very close or same to the reported value of 401 nm [16]. The quinone was separated and purified by column chromatography and the product was isolated with high yield (70%). The quinine is chracterised by melting point measurements with the value 110˚C [17].

In order to find out the reaction rate between 3,5-DTBC and **1**, the reaction kinetics was studied and observed that the time dependent change in absorbance was at a wavelength of 398 nm in methanol and 401 in acetonitrile. Gradually the colour of the solution was turned deep brown that indicates that the gradual conversion of 3,5-DTBC to 3,5-DTBQ. In methanol the difference in absorbance ΔA at 398 nm was plotted against time to calculate the initial rate for that particular catalyst to substrate concentration ratio (Fig.5). A first-order catalytic reaction was observed, with initial rate 5.08×10^{-3} min^{-1}. But in acetonitrile the same was done at 401 nm, the reaction was also of first order (Fig. 6) with initial rate 3.25×10^{-5} min^{-1}.

3.4.1. Enzyme kinetics study

Enzymatic kinetic experiments were performed UV-Vis spectrophotometrically thermostated at 25°C with the complex, and the substrate 3,5-DTBC in MeOH. 0.04 ml of each complex solution, with a constant concentration of 1×10^{-4} M, was added to 2 ml of 3,5-DTBC of a particular concentration (varying its concentration from 1×10^{-3} M to 1×10^{-2} M) to achieve the ultimate concentration of the complex as 1×10^{-4} M. The conversion of 3,-5-DTBC to 3,5-DTBQ was monitored with time at a wavelength of 398 nm for solutions in MeOH and 401 nm in acetonitrile. The rate for each concentration of the substrate was determined by the initial rate method.

The rate versus concentration of substrate data were analyzed on the basis of Michaelis-Menten approach of enzyme kinetics to get the Lineweaver-Burk (double reciprocal) plot as well as the values of the various kinetic parameters V_{max} (maximum velocity), K_M (Michaleis-Menten constant) and K_{cat} (Turn over number). The observed rate vs. [substrate] plot along with Lineweaver-Burk plot in methanol and acetonitrile solutions are given respectively in Figs. 7 and 8. The turnover numbers (K_{cat}) are calculated as 4.02×10^3 h^{-1} in methanol and 9.57×10^3 h^{-1} in acetonitrile.

3.4.2. Mechanism of catecholase activity

The catalytic process takes place in two steps. The first step is the slowest and is considered as the rate determining step. In this step 1:1 adduct of copper complex and catechol may form. The mechanistic pathway of catecholase activity was explained by mass spectral analysis of a 1:100 mixture of **1** and 3,5-DTBC. **1** was dissociated much readily and formed a mononuclear unit which is characterized by HRMS peak at 369.54 (Fig. S4(a); Supporting information). ESI MS spectrum of **1** is also given with m/z 369.97 (Fig. S4(b); Supporting information). In HRMS, m/z value at 554.66 indicates the formation of the adduct of **1** and 3,5-DTBC (Fig. S5; Supporting information).The sodium aggregate of 3,5-DTBQ was detected by HRMS peak at 244.78 (Fig. S6; Supporting information). The catalytic cycle (Scheme 3) of the catecholase activity was proposed and the probable molecular units in the cycle were characterized by HRMS (Fig. S7(a-c), Supporting information). In this process molecular oxygen oxidized 3,5-DTBC to the corresponding quinone, 3,5-DTBQ and reduced itself to hydrogen peroxide. The liberated $H_2O_2$was identified and characterized spectrophotometrically (S1; Supporting information) [18].

*3.5. Phenoxazinone synthase activity of **1**: spectrophotometric study*

The phenoxazinone synthase activity has been studied by using the substrate,*o*-aminophenol (OAPH). In presence of molecular oxygen, the oxidation of OAPH to the corresponding 2-aminophenoxazinone-3-one was catalyzed by the compound **1**. The spectral band of OAPH appears at 232 nm and 286 nm in methanol (inset to Fig. 9), 233 nm and 292nm in acetonitrile (inset to Fig. S8, Supporting information) and 238 nm and 288 nm in dichloromethane (DCM) (inset to Fig. S9, Supporting information). The solution of **1** in various solvents like, methanol, acetonitrile and dichloromethane are treated into 100 equivalent of OAPH and the repetitive UV-Vis scan was recorded. One representative scan is given in Fig.9 (other scans in MeCN and DCM are given in Fig. S8 and S9; Supporting information). The colourless solution of OAPH becomes deep brown due to the formation of APX. The characteristic peak of APX grows smoothly at ~420 nm in MeOH, MeCN and DCM (419, 423 and 416 nm, respectively) [10d]. The identification of APX was also done by HRMS at m/z value 213.80 (Fig. S10; Supporting information). The time dependent change of absorbance for the catalytic reaction was done at a wavelength 420 nm for 30 min in the above solvents to monitor the reaction kinetics and find out the initial rate between OAPH and **1**. The difference in absorbance at 420 nm is plotted against time in minute in different solvents. One representative plot (in MeOH) is given in Fig. 10 (plots in MeCN and DCM are given in Figs. S11 and S12; Supporting information).From the slope the initial rate for the particular catalyst and substrate is obtained. The initial rates are 5.43×10^{-3}, 6.14×10^{-4}, 1.53×10^{-3} min^{-1} in MeOH, MeCN and DCM, respectively.

3.5.1. Enzyme kinetic study

Enzymatic kinetic experiments were performed UV-Vis spectrophotometrically thermostated at 25°C with the complex, and the substrate OAPH in MeOH, MeCN and DCM. 0.04 ml of each complex solution, with a constant concentration of 1×10^{-4} M, was added to 2 ml of OAPH of a particular concentration (varying its concentration from 1×10^{-3} M to 1×10^{-2} M) to achieve the ultimate concentration of the complex as 1×10^{-4}M. The conversion of OAPH to APX was monitored with time at a wavelength of 420 nm for solutions in different solvents. The rate for each concentration of the substrate was determined by the initial rate method.

The rate versus concentration of substrate data were analyzed on the basis of Michaelis-Menten approach of enzymatic kinetics to get the Lineweaver-Burk (double reciprocal) plot as well as the values of the various kinetic parameters V_{max}, K_M and K_{cat} in MeOH, MeCN and DCM. Plot in MeOH is given in Fig. 11. The other plots (in MeCN and DCM) are available in Figs. S13 and S14; Supporting information). The turnover numbers (K_{cat}) are 1.065×10^3 h^{-1} in MeOH, 2.13×10^2 h^{-1} in MeCN and 2.844×10^3 h^{-1} in DCM.

3.5.2. Mechanism of phenoxazinone synthase activity

To predict the mechanistic pathway of phenoxazinone synthase activity of **1**, it is found that initially OAPH forms an adduct with **1** which is identified by mass spectrometry at m/z = 847.30 (OAPH-**1**) (Fig. S15; Supporting information). This adduct generates 2-amoinophenoxazine-3-one through some intermediate reaction with molecular oxygen. Reduced molecular oxygen in the form of H_2O_2 was detected spectrophotometrically (S1; Supporting information) [18].

4. Conclusion

We have synthesized and X-ray crystallographically characterized a new antiferromagnetically coupled dinuclear copper(II) complex **1**. **1** was found to catalyze separately the aerial oxidation of 3,5-ditertiarybutyl catechol to its corresponding quione and *o*-aminophenol to phenoxazinone chromophore. The turn over number for the catecholase activity by **1** in methanol and acetonitrile solvent was better than that of the other reported dinuclear copper complexes [4, 5(a), 5(b), 6(a)]. Similarly the turn over number in phenoxazinone synthase activity by **1** in different solvents is appreciable, sometimes better than few reported ones [2(a), 9(a), 9(b)]. Henece compound **1** we reported may be regarded as a good addition to the catecholase mimic dinuclear copper(II) complex.

5. Supplementary data

CCDC 1572023 contains the supplementary crystallographic data for **1**. This data can be obtained free of charge via http://www.ccdc.cam.ac.uk/conts/retrieving.html, or from the Cambridge Crystallographic Data Centre, 12 Union Road, Cambridge CB2 1EZ, UK; fax: (+44) 1223-336-033; or e-mail: deposit@ccdc.cam.ac.uk.

Acknowledgement

RG is thankful to Department of Science & Technology, Government of West Bengal [No. 781(Sanc.)/ST/P/S&T/4G-4/2013 dated 04-12-2014], India for financial assistance. AKG thanks CSIR, New Delhi for his fellowship. Different infrastructural facilities at our university provided by PURSE programme, DST, Govt of India is gratefully acknowledged.

Table 1 – Crystal data and structure refinement parameter of compound **1**

Emperical formula	$C_{32}\ H_{32}N_2O_2S_2Cl_2Cu_2$
Formula weight	738.74
T (K)	293(2)
Wavelenght (Å)	0.71073
Crystal system	Monoclinic
Space group	*P121/n1*
Unit cell dimensions	
a (Å)	12.556(5)
b (Å)	7.677(5)
c (Å)	16.653(5)
α (˚)	90
β (˚)	93.037(5)
γ (˚)	90
V(Å^3)	1603.0(13)
Z	4
D_{calc}(mg m^{-3})	1.535
Absorption coefficient(mm^{-1})	1.656
F(000)	760
Crystal size (mm^3)	0.42 × 0.31 × 0.24
Theta range for data collection (˚)	1.98-30.58
Index ranges	$-17 \le h \le 17$, $-10 \le k \le 10$, $-23 \le l \le 23$
Reflections collected	16850
Independent reflections	4882 [Rint= 0.0289]
Completeness of theta	99.4 % [θ=30.58]
Absorption correction	Multi-scan
T_{max} and T_{min}	0.7461 and 0.5134
Refinement method	Full matrix
Data/restrains/parameters	4882/0/190
Goodness-of fit (GOF) F^2	1.032

Final *R* index [$l > 2\sigma(l)$]	R_1= 0.0407 and wR_2=0.1110
R index (all data)	R_1= 0.0659 and wR_2=0.1423
Largest difference between peak and hole (e Å^{-3})	0.463, -0.659

Table 2 – Bond lengths (Å) and bond angles (°) of **1**

Bond lengths			
Cu(1)-O(1)	1.8920(18)	Cu(1)-Cl(1)	2.2860(9)
Cu(1)-N(1)	1.953(2)	Cu(1)-Cl(1')	2.815
Cu(1)-S(1)	2.3569(10)		
Bond angles			
O(1)-Cu(1)-N(1)	93.21(9)	O(1′)-Cu(1′)-N(1′)	93.21(9)
O(1)-Cu(1)-Cl(1)	92.78(6)	O(1′)-Cu(1′)-Cl(1′)	92.78(6)
N(1)-Cu(1)-Cl(1)	173.15(7)	N(1′)-Cu(1′)- Cl(1′)	173.15(7)
O(1)-Cu(1)-S(1)	158.84(7)	O(1′)-Cu(1′)-S(1′)	158.84(7)
N(1)-Cu(1)-S(1)	85.71(7)	N(1′)-Cu(1′)-S(1′)	85.71(7)
Cl(1)-Cu(1)-S(1)	89.90(3)	Cl(1′)-Cu(1′)-S(1′)	89.90(3)

References

[1] (a) I. A. Koval, P. Gamez, C. Belle, K. Selmeczi, J. Reedijk, Chem. Soc. Rev., 35 (2006) 814-840; (b) S. K. Dey, A. Mukherjee, Coord. Chem. Rev. 310 (2016) 80-115; (c) P. Comba, B. Martin, A. Muruganantham, J. Straub, Inorg. Chem. 51 (2012) 9214-9225; (d) J. Reim, B. Krebs, J. Chem. Soc., Dalton Trans., (1997) 3793-3804.

[2] (a) A. Panja, P. Guionneau, Dalton Trans., 42 (2013) 5068-5075; (b) M. Mitra, R. Ghosh, Indian J. Chem., 55A (2016) 681-685.

[3] T. Klabunde, C. Eicken, J. C. Sacchettini, B. Krebs, Nat. Struct. Biol., 5 (1998) 1084.

[4] (a) E. Monzani, G. Battaini, A. Perotti, L. Casella, M. Gullotti, L. Santagostini, G. Nardin, L. Randaccio, S. Geremia, P. Zanello, G. Opromolla, Inorg. Chem., 38 (1999) 5359-5369; (b) S. Torelli, C. Belle, I. Gautier-Luneau, J. L. Pierre, E. Saint-Aman, J. M. Latour, L. Le Pape, D. Luneau, Inorg. Chem., 39 (2000) 3526-3536; (c) C. Belle, C. Beguin, I. Gautier-Luneau, S. Hamman, C. Philouze, J. L. Pierre, F. Thomas, S. Torelli, E. Saint-Aman, M. Bonin, Inorg. Chem., 41 (2002) 479-491.

[5] (a) C. -T. Yang, M. Vetrichelvan, X. Yang, B. Moubaraki, K. S. Murray, J. J. Vittal, Dalton Trans., (2004) 113-121; (b) M. Merkel, N. Möller, M. Piacenza, S. Grimme, A. Rompel, B. Krebs, Chem. Eur. J., 11 (2005) 1201-1209; (c) B. Sreenivasulu, F. Zhao, S. Gao, J. J. Vittal, Eur. J. Inorg. Chem., (2006) 2656-2670; (d) S. Mukherjee, T. Weyhermuller, E. Bothe, K. Wieghardt, P. Chaudhuri, Dalton Trans., (2004) 3842-3853; (e) A. Sarkar, A. K. Ghosh, V. Bartolasi, D. Ray, Dalton Trans., 41 (2012) 1889-1896.

[6] (a) Y. Thio, X. Yang, J. J. Vittal, Dalton Trans., 43 (2014) 3545-3556; (b) S. Majumder, S. Mondal, P. Lemoine, S. Mohanta, Dalton Trans., 42 (2013) 4561-4569; (c) M. Mitra, P. Raghavaiah, R. Ghosh, New J. Chem., 39 (2015) 200-205; (d) P. Vijayan, P.

Viswanathamurti, K. Velmurugan, R. Nandhakumar, M. D. Balakumaran, P. T. Kalaichelvan, J. G. Malecki, RSC Adv., 5 (2015) 103321-103342, (e) S. Dasgupta, J. Adhikary, S. Giri, A. Bauza, A. Frontera, D. Das, Dalton Tans., 46 (2017) 5888-5900.

[7] (a) S. Anbu, M. Kandaswami, Polyhedron 30 (2011) 123-131; (b) S. Anbu, E. C. B. A. Alegria, A. J. L. Pombeiro, Inorg. Chim. Acta (2014) 431 (2015) 139-144; (c) S. Anbu, A. Paul, A. P. C. Ribeiro, M. F. C. Guedes da Silva, M. L. Kuznetsov, A. J. L. Pombeiro, Inorg. Chim. Acta 450 (2016) 426-436.

[8] A. W. Smith, A. Camara-Artigas, M. Wang, J. P. Allen, W. A. Francisco, Biochemistry, 45 (2006) 4378-4387.

[9] (a) M. R. Maurya, S. Sikarwar, T. Joseph, S. B. Halligudi, J. Mol. Cat. A: Chemical, 236 (2005)132-138; (b) F. Bruyneel, O. Payen, A. Rescigno, B. Tinant, J. Marchand-Brynaert, Chem. Eur. J., 15 (2009) 8283-8295; (c) C. Mukherjee, T. Weyhermüller, E. Bothe, E. Rentschler, P. Chaudhuri, Inorg. Chem., 46 (2007) 9895-9905; (d) T. M. Simándi, Z. May, I. C. Szigyártó, L. I. Simándi, Dalton Trans., (2005) 365-368.

[10] (a) A. Panja, A. Shyamal, A. Saha, T. K. Mandal, Dalton Trans., 43 (2014) 5443; (b) A. Panja, Dalton Trans., 43 (2014) 7760; (c) A. Panja, RSC Adv., 4 (2014) 37085; (d) M. Mitra, T. Kundu, G. Kaur, G. Sharma, A. R. Choudhury, Y. Singh, R. Ghosh, RSC Adv., 6 (2016) 58831.

[11] Bruker (2007). SMART, SAINT and SADABS. Bruker AXS Inc., Madison, Wisconsin, USA.

[12] G. M. Sheldrick, 1999 SHELXL-97, University of Göttingen, Göttingen, Germany.

[13] K. Nakamoto, Infrared and Raman Spectra of Inorganic and Coordination Compounds, part B: Applications in Coordination, Organometallic, and Bioinorganic Chemistry, John Wiley & Sons Inc, New Jersey, 2009.

[14] (a) S. Parimala, K. N. Gita, M. Kandaswamy, Polyhedron, 17 (1998) 3445-3453; (b) J. Mukherjee, R. Mukherjee, Inorg. Chim. Acta., 337 (2002) 429-438.

[15] A. Pal, B. Biswas, S. K. Mondal, C. -H. Lin, R. Ghosh, Polyhedron, 31 (2012) 671-675.

[16] F. Zippel, F. Ahlers, R. Werner, W. Haase, H.-F. Nolting, B. Krebs, Inorg. Chem., 35 (1996) 3409.

[17] S. Tsuruya, S.-I. Yanai and M. Masai, Inorg. Chem., 25 (1986) 141.

[18] A. I. Vogel, Textbook of Quantitative Inorganic Analysis, 3rd ed., Longmans, Green and Co. Ltd, London, 1961. p. 366.

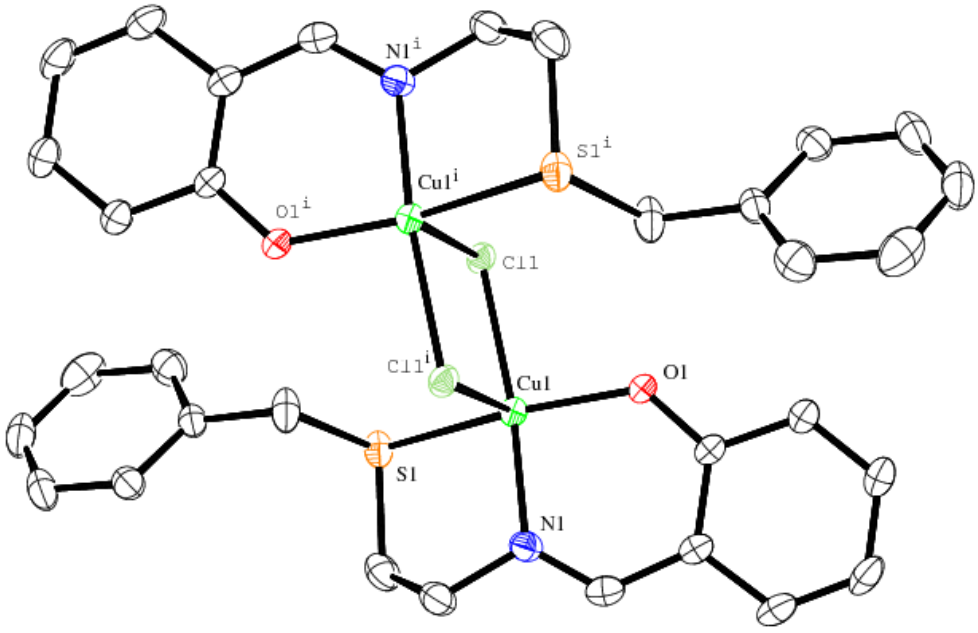

Fig. 1 – ORTEP of **1** with 30% ellipsoid probability

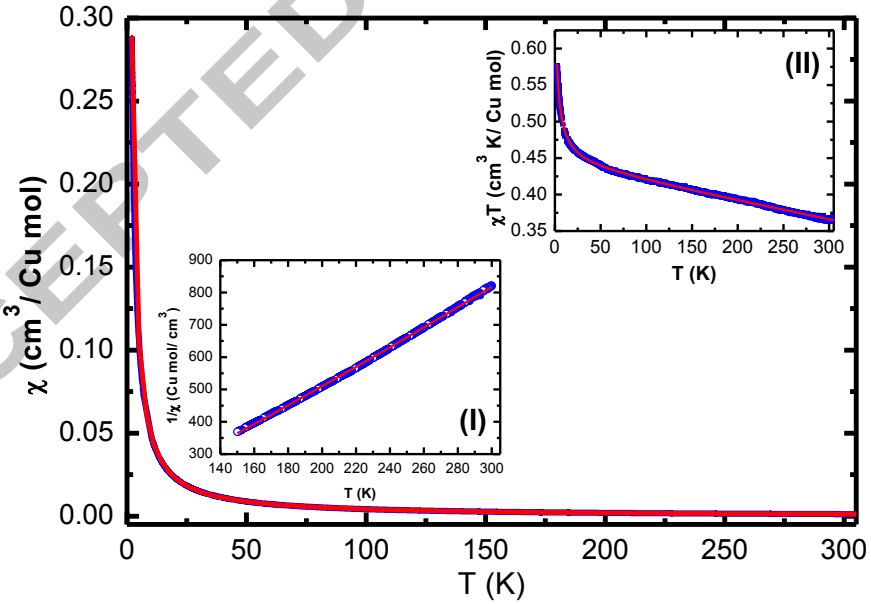

Fig. 2 – Plot of χ(T) vs T of complex **1** [inset I: 1/χvs T and inset II: χTvs T]

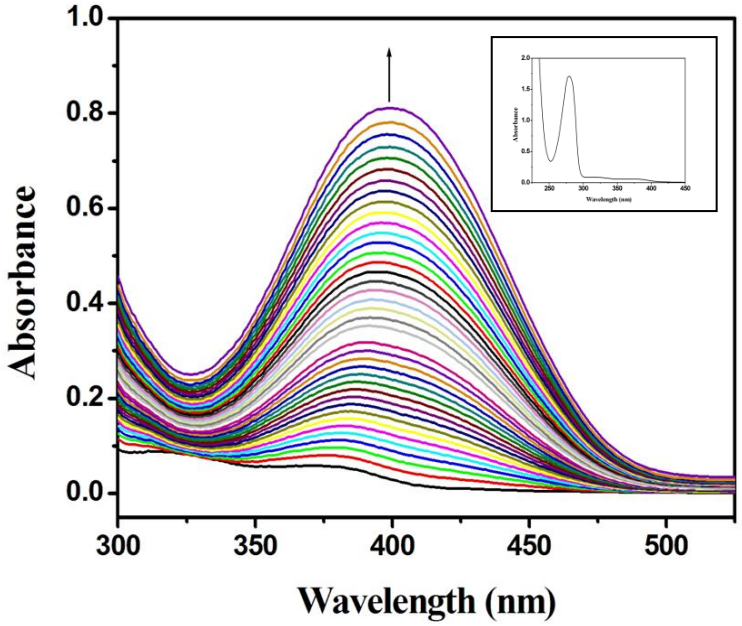

Fig. 3 – Change in spectral pattern of complex **1** after reaction with 3,5-DTBC, observing the reaction for 6 h in methanol [inset: spectrum of pure 3,5-DTBC in methanol]

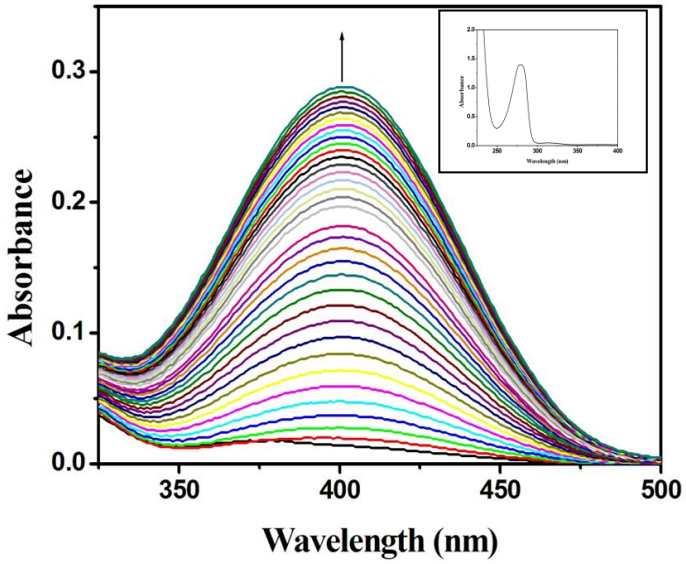

Fig. 4 – Change in spectral pattern of complex **1** after reaction with 3,5-DTBC, observing the reaction for 6 h in acetonitrile [inset: spectrum of pure 3,5-DTBC in acetonitrile]

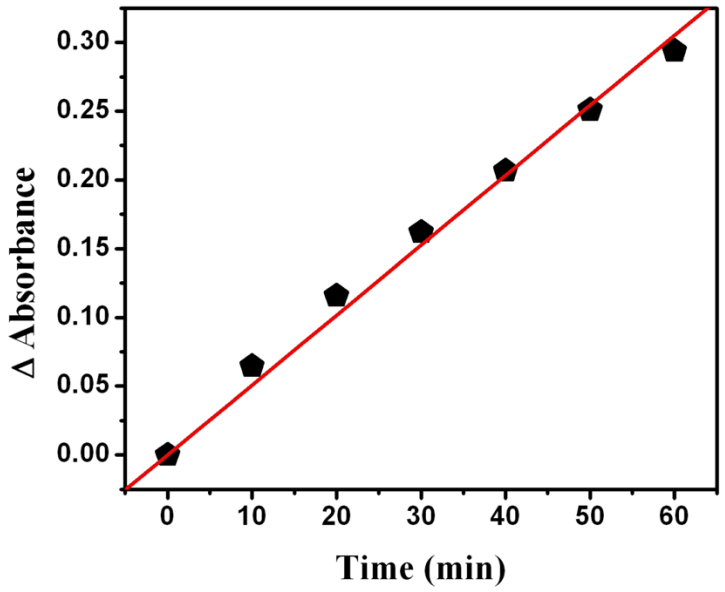

Fig. 5 – A plot of the difference in absorbance (ΔA) vs time to evaluate the rate of catalysis of 3,5-DTBC by **1** in MeOH

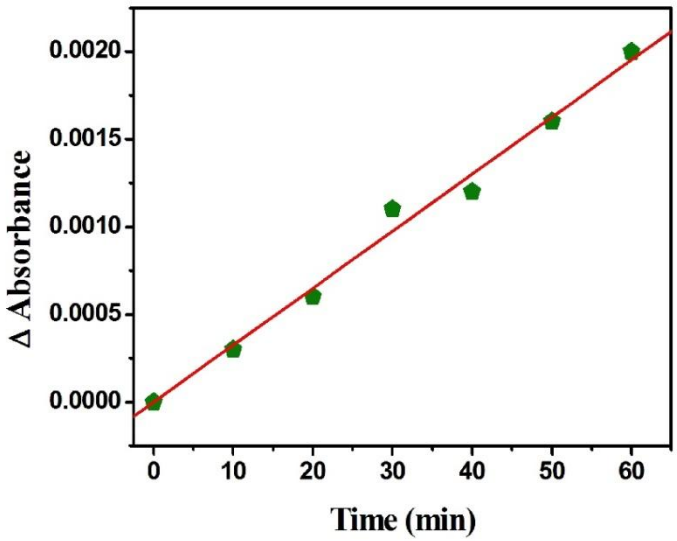

Fig. 6 – A plot of the difference in absorbance (ΔA) vs time to evaluate the rate of catalysis of 3,5-DTBC by **1** in MeCN

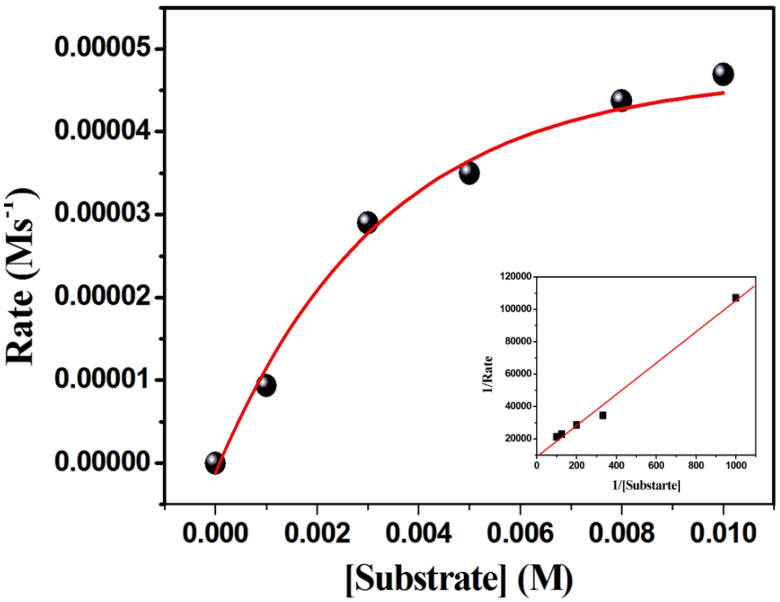

Fig. 7 – Plot of rate vs. [substrate] (3,5-DTBC) in presence of **1** in MeOH [inset: Lineweaver-Burk plot]

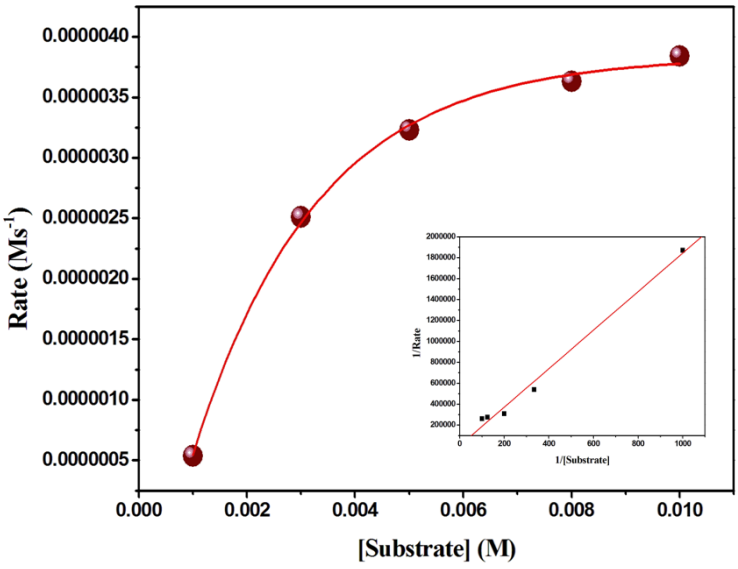

Fig. 8 – Plot of rate vs. [substrate] (3,5-DTBC) in presence of **1** in MeCN [inset: Lineweaver-Burk plot]

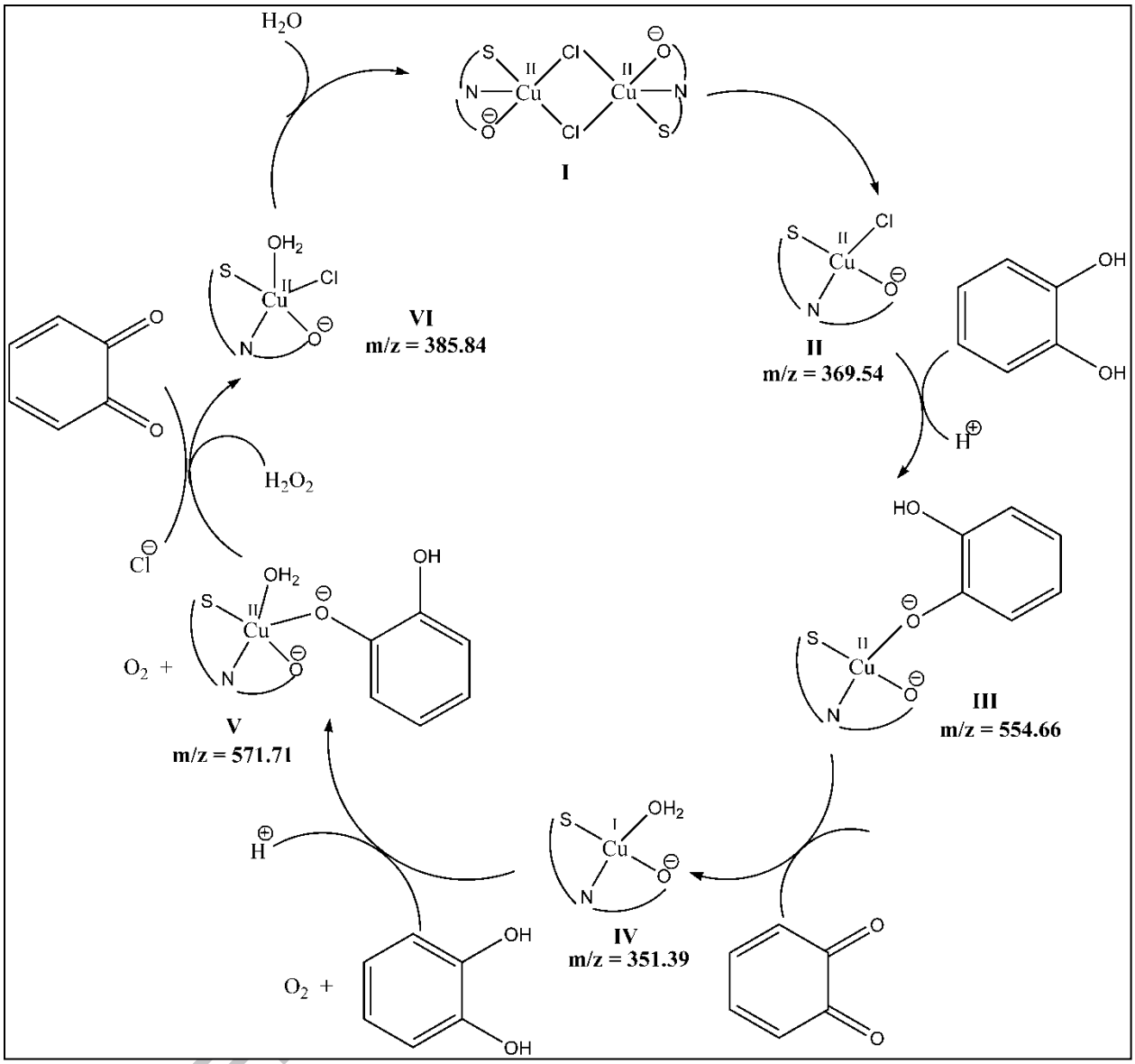

Scheme 3 – Catalytic cycle for catecholase activity by **1**

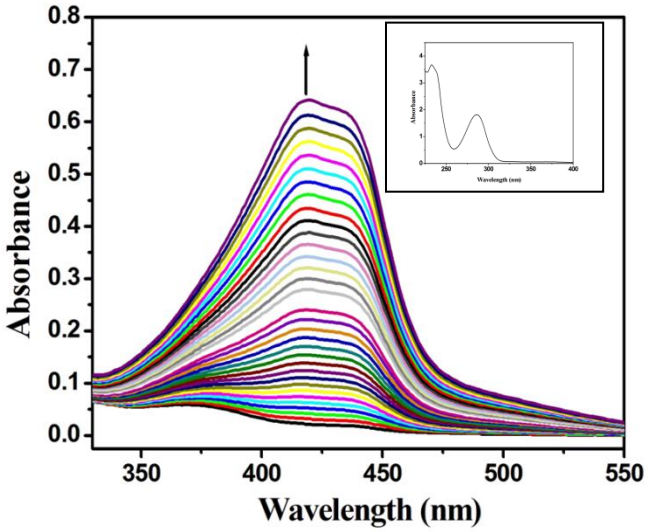

Fig. 9 – Change in spectral pattern of complex **1** after reaction with OAPH, observing the reaction for 6 h in methanol [inset: spectrum of pure OAPH in methanol]

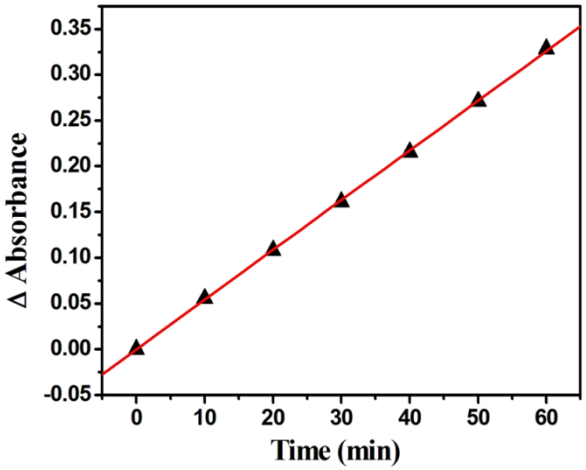

Fig. 10– A plot of the difference in absorbance (ΔA) vs time to evaluate the rate of catalysis of OAPH by **1** in methanol

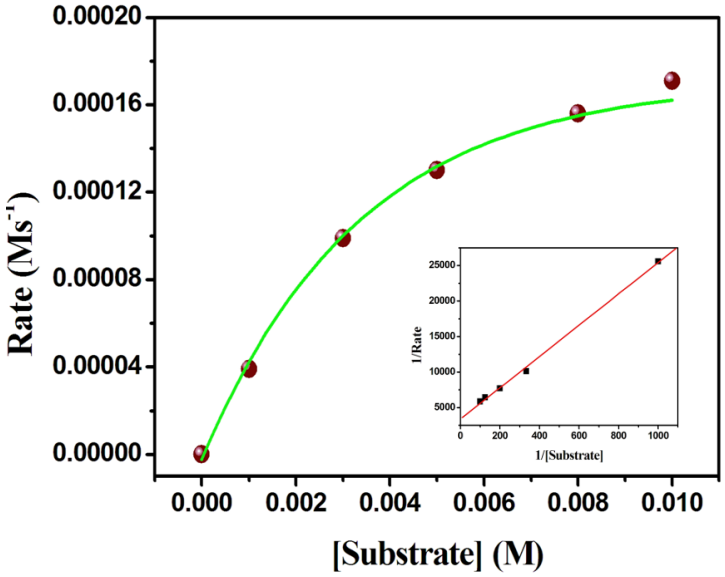

Fig. 11 – Plot of rate vs. [substrate] (OAPH) in presence of **1** in MeOH [inset: Lineweaver-Burk plot]

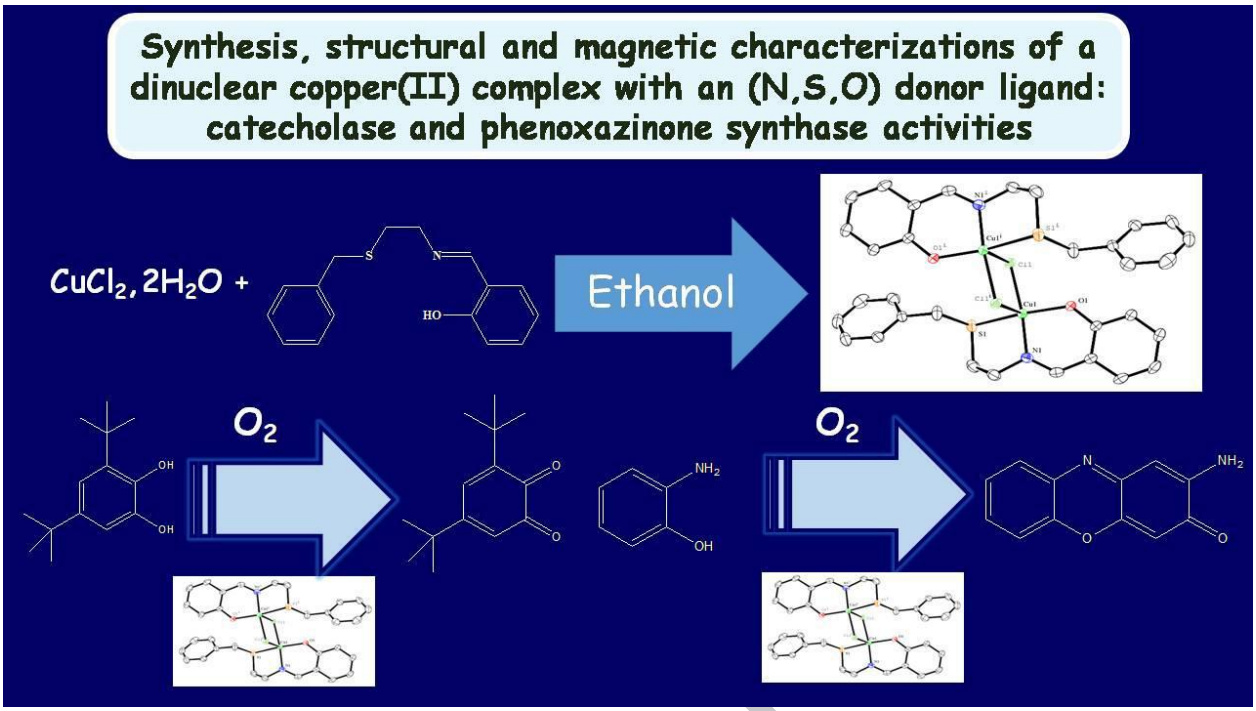

A weakly ferromagnetically coupled dinuclear Cu(II) complex with square pyramidal geometry at each metal centre was synthesized and crystallographically characterized. The compound was found to had catecholase and phenoxazinone synthase-like activities in different solvents with appreciable turn over number.

Highlight

- Dinuclear Cu(II) complexes
- Schiff base
- Catecholase activity
- Phenoxazinone synthase activity